Rock Fragmentation by Blasting – Sanchidrián (ed)
© 2010 Taylor & Francis Group, London, ISBN 978-0-415-48296-7

The extent of blast damage from a fully coupled explosive charge

S.R. Iverson, W.A. Hustrulid, J.C. Johnson, D. Tesarik & Y. Akbarzadeh
NIOSH Spokane Research Laboratory, Spokane, WA, USA

ABSTRACT: The Spokane Research Laboratory (SRL) of the U.S. National Institute of Occupational Safety and Health (NIOSH) is developing a "damage-radius" based drift round blast design procedure as part of a research program aimed at improving ground control for mines using the drill and blast excavation method. The overall program goal is to minimize the amount of unwanted damaged to the perimeter of excavations from blasting and reduce ground fall-related fatalities and injuries through the implementation of a practical, yet technically sound, design procedure. An experiment was performed to investigate the damage zone resulting from a single blasthole charged with a conventional mining explosive. A concrete block was instrumented with an array of embedded strain gages grouted at various distances from the blasthole. After the blast, the extent of the damage zone was quantified using these strain gage readings and by a variety of other techniques including a Micro-Velocity Probe, P-wave and tensile testing of the recovered core, laser scanning of the block surface and visual examination of the interior of the block using wire saw cuts. Predictions of blast damage were made using various blast damage models. These models including the modified-Ash, NIOSH stress decay, Drukovanyi stress, NIOSH-modified Holmberg-Persson, and a Hydrodynamic based approach. The results from each model were compared to the experimental results. This paper describes the results from the concrete block experiment and the various damage models.

1 INTRODUCTION

The mission of the Spokane Research Laboratory (SRL) of the U.S. National Institute for Occupational Safety and Health (NIOSH) is to provide quality leadership in the prevention of work-related illnesses, injury, and death in the extractive industries in the western United States. One specific goal of the NIOSH mining program is to reduce underground fatalities and injuries due to ground falls. Aggressive blasting is common in the industry, with the result being overbreak, radial fracturing into the rock mass, loosening of existing fractures, damage to existing ground support, and poorly shaped openings. Through the use of well-designed cautious blasting procedures, ground control in mines can be markedly improved. The increased use of cautious blasting in the industry could improve ground quality which translates into improved safety for the miner.

As part of its program to advance cautious blasting principles, NIOSH has developed a "damage-radius" based design procedure (Hustrulid & Johnson 2008). The design approach incorporates accurately placed fully coupled buffer charges and decoupled perimeter charges. In order to control perimeter damage, both the fully coupled buffer charge and the perimeter charge damage radii are needed for design. The block test experiment described in this paper provides a method to validate damage caused by fully coupled charges used either as a buffer charge or as a perimeter charge. This paper presents five different blast models currently under assessment for possible inclusion in a careful blasting design software tool.

Note: Mention of any company or product name does not constitute endorsement by the National Institute for Occupational Safety and Health (NIOSH) or the U.S. Government.

2 CONCRETE BLOCK EXPERIMENT

The concrete block experiment comprises a large concrete block measuring 2.4 m wide by 2.4 m long and 1.5 m high, a single blasthole, and an array of strain gage sensors to measure radial strain verses distance. The concrete block is intended to represent a homogeneous rock mass without structure. The concrete block is shown in Figure 1 prior to blasting. Physical properties are listed in Table 1.

The blasthole (38 mm diameter) was percussion-drilled, nearly horizontal, and had a length of 1.8 m. It was collared at block mid-height with a burden of 45 cm. The blasthole was charged using Dyno® AP (Dyno Nobel 2009). The explosive was tamped creating a fully coupled charge 1.2-m long measured from the hole-bottom.

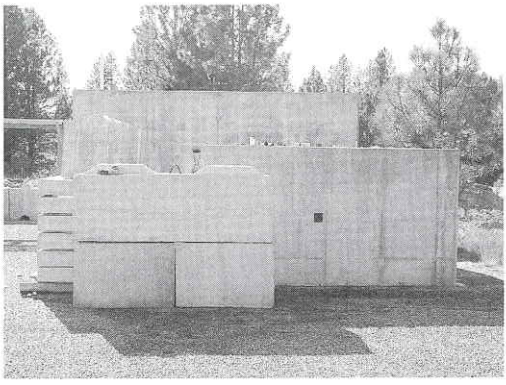

Figure 1. Photograph of block experiment prior to test showing placement of barrier blocks to restrain fly rock.

Table 1. Physical properties of the concrete block.

Parameter	Value
Cohesion, MPa	4.9
Internal friction angle, degrees	43
Uniaxial compressive strength, MPa	21
Tensile strength, Brazilian, MPa	1.75
Young's modulus, static, GPa	13.1
Young's modulus, dynamic, GPa	18.6
Poisson's ratio	0.25
Speed of sound, bar, m/sec	2800
Speed of sound, block, m/sec	3100
Density, kg/m^3	2000
Crushing Decay γ, 1/cm	0.12
Transition Decay β, 1/cm	0.03
Seismic Decay α, 1/cm	0.0005
Dynamic Strength $\sigma_{\beta\gamma}$, MPa	48
Dynamic Strength $\sigma_{\alpha\beta}$, MPa	22

The charge extended to a distance of 0.6 m from the collar. Table 2 lists the properties for Dyno® AP explosive.

An array of strain gages allows measurement of strain attenuation with distance from the charge. These data are used to validate certain aspects of the blast models described later. Strain gage rosettes were embedded in the concrete at the same height as the blasthole. Instrument emplacement holes were diamond drilled at the appropriate locations to record the propagation of stresses and strains. The strain gage rosettes were first bonded to the bottom ends of cured rectangular grout bars and the assembly was then grouted in the holes using the same grout. The grout had similar acoustic properties as the concrete to limit wave reflection. The instrument emplacement holes were drilled at intervals of 23 cm away from the blasthole. A generalized plan view of the block experiment is shown in Figure 2.

Although a rectangular grid of three strain gages was used at each location, results from only the center, or radial strain gage were used. Each strain gage was connected to one arm of a Wheatstone bridge (quarter bridge configuration). The bridge output was connected to a Genesis data recorder manufactured by LDS Test and Measurement, Inc. Data were collected at the maximum rate of 1 MHz.

Table 2. Properties of the Dyno® AP explosive.

Parameter	Value
Explosive density, g/cc	1.15
Detonation velocity, m/sec	4700*
Explosive diameter, mm	31.75
Tamped diameter, mm	38.1
Relative weight strength**	0.88
Relative bulk strength**	1.00
Charge concentration, kg/m	1.31
Tamped charge length, m	1.22
Total charge weight, kg	1.60
Energy, cal/g	775
Gas volume, moles/kg	41
Ratio of specific heats	3

* unconfined at 32 mm diameter.
** ANFO = 1.00 @ 0.82 g/cc (Dyno Nobel 2009).

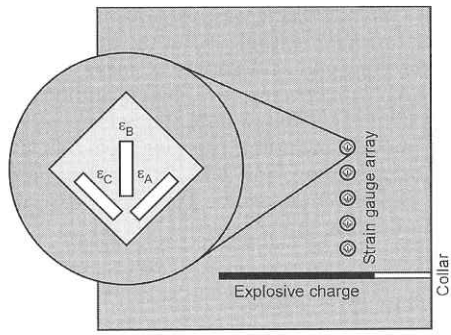

Figure 2. Top view of block showing the locations of the strain gage array and the blasthole.

3 EXPERIMENTAL RESULTS

3.1 *Damage measurement*

Visual damage patterns were quantified using a laser scanner to map crack surfaces exposed as the loosened material was scaled. Figure 3 shows one view of the block surface after final scaling.

An NX (78 mm diameter) inspection hole was diamond drilled through the block and the core collected for testing. The hole was drilled horizontal and normal to the blasthole axis. The end of the inspection hole day-lighted 5 cm below the remaining half-barrel of the blasted surface.

A bore hole camera was used for visual inspection of the NX hole. One radial crack was

identified at between 60 cm and 70 cm away from the blasthole position. This crack was confirmed in the Micro-Velocity Probe (MVP) data shown in Figures 5 and 6.

Three wire saw cuts were made normal to the blasthole at distances of 0.69-m, 1.22-m, and 1.60-m from the blasthole collar. Radial cracks were easily identified on the wire saw cut surfaces. The cracks were highlighted with a permanent marker laser scanned, digitized, and exported as a profile into AutoCAD. The crack profile from the first cut at 0.69-m measured from the blast hole collar is shown in Figure 4. This cut aligns closely with the embedded strain gage array. A radial crack limit of 1.76-m was measured and six major radial cracks were identified.

Prior to wire sawing, the MVP, developed by ESG Solutions, was inserted into the inspection hole and measurements were made at various intervals. In the test configuration used, the separation distance between the transmitter and receiver shear crystals was a nominal 10 cm. Calibration of the system was performed using a cast aluminum cylinder. Two different orientations of the transducers were used; vertical and horizontal. The time required for the generated shear wave to traverse the 10 cm distance between the transmitter and the receiver was measured using a Tektronix TDS 1001B digital oscilloscope. The first measurement was made with the MVP positioned just inside the collar. Subsequent measurements were then made at intervals of generally 2.5 cm both into and out of the hole. The results are shown in Figures 5 and 6 for the two MVP orientations. The location of the major crack is clearly seen in both records. An exponential regression curve fit of the data was applied and a damage limit of 50 cm is indicated at 95 pct of the measured background velocity for each orientation.

Ultrasonic measurements were conducted on the NX core using a University of Utah designed cross-core P-wave measurement device (McCarter 2006). The core was placed in a special holder and the transmitter and receiver transducers oriented across the diameter. The time required for a P-wave to traverse the diameter was recorded. From the data, a plot of sonic velocity as a function of distance from the blasthole was constructed (Figure 7). An exponential curve fit of the data was applied and a damage limit of 50 cm is indicated at 95 pct of the measured background velocity.

Brazilian tests were performed on cut sections of the NX core following testing procedure ASTM

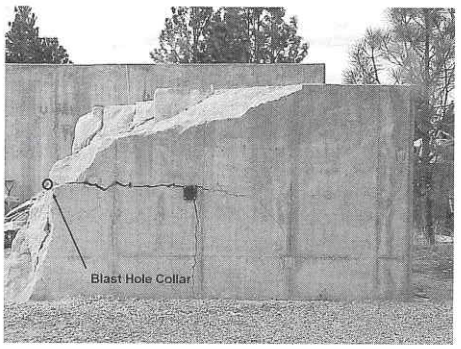

Figure 3. Tested block after scaling showing location of blasthole collar.

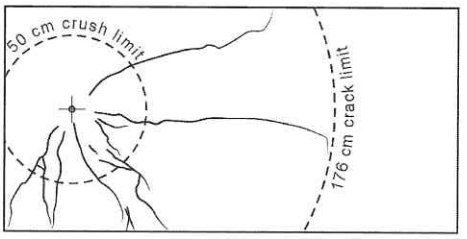

Figure 4. Internal inspection by wire saw cut exposed the radial crack damage. The measured crush and crack limits are shown for comparison.

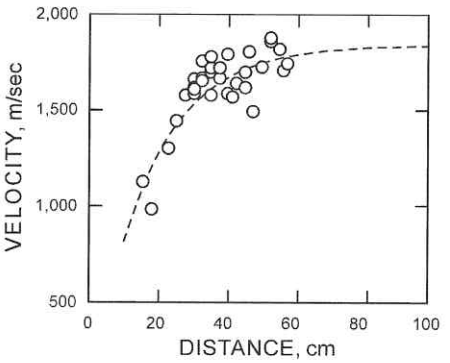

Figure 5. Shear wave velocity as a function of distance from the blasthole with sensors oriented vertically.

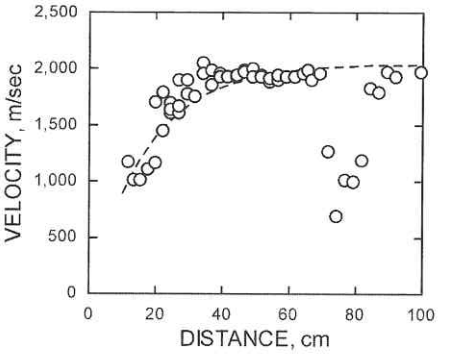

Figure 6. Shear wave velocity as a function of distance from the blasthole with sensors oriented horizontally.

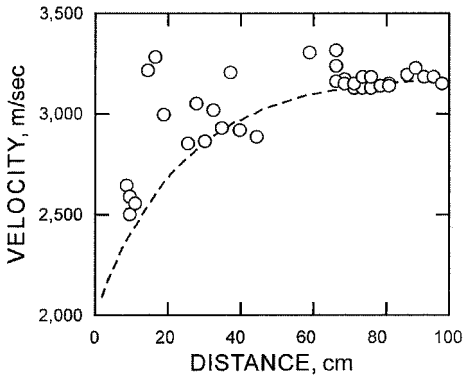

Figure 7. P-Wave velocity across the inspection core diameter as a function of distance from the blasthole.

D 3967 (2001) using rigid seating. The discs were nominally 5.2 cm in diameter and 2.2 cm thick or a thickness to diameter ratio of 0.42. Splitting tensile strength was computed using,

$$\sigma_t = \frac{2P}{\pi LD} \quad (1)$$

where P = Maximum applied load, L = length of the specimen, D = diameter of the specimen, σ_t = splitting tensile strength.

The average splitting tensile strength σ_t for specimens further that 70 cm from the blasthole was 1.75 MPa. This is considered the undamaged strength. Figure 8 shows the splitting tensile strength versus distance from the blasthole. An exponential regression curve fit of the data was applied and a damage limit of 50 cm is indicated at 95 pct of the measured background strength.

3.2 *Strain measurement*

Table 3 lists the peak amplitude of the compressive radial strain measured by radial strain gages at each of the five instrument holes in the concrete block. A common parameter often used to measure damage is the peak particle velocity (PPV). Hustrulid (1999) gives the general relationship between the particle velocity and wave velocity. From the maximum strain the PPV can be computed using,

$$PPV = c\varepsilon \quad (2)$$

where c = velocity of sound in the block that is 3100 m/s from Table 1. The peak radial stress is estimated using the product of the peak radial strain and the dynamic Young's modulus of the rock.

$$\sigma = E_{dyn}\varepsilon \quad (3)$$

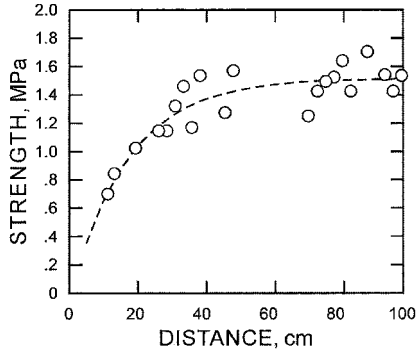

Figure 8. Splitting tensile strength as a function of distance from the blasthole.

Table 3. Concrete block peak measured strain values converted to PPV and stress.

Distance, cm	Peak strain	PPV, m/s	Peak radial stress, MPa
22.9	.006475	20.1	120.4
45.7	.001592	4.9	29.6
68.6	.000691	2.1	12.9
91.4	.000332	1.0	6.2
114.3	.000288	0.9	5.4

where E_{dyn} = 18.6 GPa as listed in Table 1, σ = calculated stress, and ε = the measured strain. Table 3 lists the maximum measured compressive radial strains and their conversions into PPV and peak radial stress.

3.3 *Velocity of detonation measurement*

The velocity of detonation (VOD) for the explosive was not measured for this block test. A VOD measurement was however made for a subsequent block test where the same explosive and loading method were used. The measured VOD of 4,300 m/sec is lower than the reported VOD of 4,700 m/sec (Dyno Nobel 2009). The VOD measurement was made using a Handitrap II data recorder.

4 BLAST DAMAGE MODELS

Five blast damage models are described that provide either damage limits or expected PPV values associated with measured damage surrounding the charge. The models are tested using the block experiment damage results described in Section 3.1.

4.1 *The modified Ash approach*

For open pit mining applications, Ash (1963) has suggested the following relationship between the

burden (B) and the hole diameter (d_h) for fully-coupled explosives.

$$B = K_B\, d_h \tag{4}$$

where K_B = constant.

Ash (1963) found that when using ANFO (with a density of 0.82 g/cm^3) to blast average rock (density of 2.65 g/cm^3), the use of $K_B = 25$ provided very satisfactory results. When using explosives of greater bulk strength (energy/volume) than ANFO to blast the average rock, one would use $K_B = 30$ or even $K_B = 35$. For surface blast design, Hustrulid (1999) recommended that designers think in terms of cylindrical fragmented plugs of rock surrounding each hole. For the "just-touching" scenario, the radius of influence (R) of the plug is equal to $B/2$.

For the present application, it will be assumed that the damage radius is equal to the radius of influence. Hence,

$$R_d/r_h = K_B \tag{5}$$

It is important to have an expression for R_d that can be applied to different explosive—rock combinations. Based upon energy considerations, Hustrulid (1999) has shown that

$$R_d/r_h = 25\sqrt{\frac{\rho_e\, s_{ANFO}}{\rho_{ANFO}}}\sqrt{\frac{2.65}{\rho_{rock}}} \tag{6}$$

where ρ_e = explosive density (g/cm^3), ρ_{rock} = rock density (g/cm^3), s_{ANFO} = weight strength with respect to ANFO, and ρ_{ANFO} = ANFO density (g/cm^3). Equation 6 can be re-written as

$$R_d/r_h = 25\sqrt{RBS}\sqrt{\frac{2.65}{\rho_{rock}}} \tag{7}$$

where RBS = relative bulk strength of the explosive with respect to ANFO expressed as a ratio. In this particular case, $RBS = 1.24$ and the density for the concrete block is $\rho_{rock} = 2.0$ g/cm^3.

Using the energy-based relationship (Equation 7) one finds

$$R_d/r_h = 25\sqrt{RBS}\sqrt{\frac{2.65}{\rho_{rock}}} = 25\sqrt{1.24}\sqrt{\frac{2.65}{2.00}} = 32$$

and thus, $R_d = 61$ cm.

Another option is to relate the damage radius to the explosion pressure for a fully coupled charge rather than to the explosive energy. The expression is given below

$$R_d/r_h = 25\sqrt{\frac{P_{e\,Exp}}{P_{e\,ANFO}}}\sqrt{\frac{2.65}{\rho_{rock}}} \tag{8}$$

where $P_{e\,Exp}$ = explosion pressure for the explosive and $P_{e\,ANFO}$ = explosion pressure for ANFO.

For practical purposes it has been found that the explosion pressure (P_e) can be approximated by

$$P_e = \frac{\rho_e (VOD)^2}{8} \tag{9}$$

where ρ_e = explosive density, kg/m^3, and VOD = velocity of detonation (km/sec). The approximate explosion pressure is,

$$P_e = \frac{P_d}{2} = 2{,}660\text{MPa}$$

Using the explosion pressure-based relationship (Equation 8) one finds

$$R_d/r_h = 25\sqrt{\frac{P_{e\,Exp}}{P_{e\,ANFO}}}\sqrt{\frac{2.65}{\rho_{rock}}} = 25\sqrt{\frac{2660}{1050}}\sqrt{\frac{2.65}{2.00}} = 48.5$$

and thus $R_d = 87$ cm. The value for $P_{e\,ANFO} = 1050$ MPa applies for the 38 mm diameter blast hole.

4.2 *NIOSH stress decay approach*

This model calculates the compressive radial stress generated by the explosive and its decay through the rock mass until it reaches its dynamic strength.

Because the explosive charge was fully coupled to the concrete block, the explosion pressure (P_e) is equal to the blasthole wall pressure (P_w) that is given by Equation 9.

The explosion pressure generates a radial stress in the concrete block that decays by two terms; geometric spreading and damage. Johnson (2009) presents three piecewise continuous functions that describe the decay of stress in the crush, transition, and seismic zones.

Equations 10 and 11 describe the damage zones, extensive and transition, while the third equation (Eq. 12) describes the undamaged elastic or seismic zone. The material properties necessary to determine the zone boundaries are the decay rates and the dynamic strengths. These properties are listed in Table 2 and were found experimentally using a laboratory test described by Johnson (2009).

The decay of stress in the crush zone is,

$$\sigma = P_w\sqrt{\frac{R_h}{R}}e^{-(R-R_h)\gamma} \tag{10}$$

where γ is the crushing damage decay constant, R_h is the blasthole radius, R is the distance from the

center of the charge, and σ is the associated stress at distance R.

Setting $\sigma = \sigma_{\beta\gamma}$, the associated stress or crushing strength listed in Table 1, and substituting the remaining dynamic properties from Table 1, R in Equation 10 becomes $R_{\beta\gamma}$, the distance to the end of the crushed zone boundary shown as

$$48 = 2660\sqrt{\frac{3.8}{R_{\beta\gamma}}}e^{-(R_{\beta\gamma}-3.8)(0.12)}$$

This equation contains one unknown that occurs in both terms and is solved numerically giving, $R_{\beta\gamma} = 26$ cm. However, this is not the final damage distance since the crushing strength must now decay through the transition zone to the seismic zone where the damage ends. The decay of stress in the transition zone is,

$$\sigma = \sigma_{\beta\gamma}\sqrt{\frac{R_{\beta\gamma}}{R}}e^{-(R-R_{\beta\gamma})\beta} \tag{11}$$

where β is the transition damage decay constant.

Setting $\sigma = \sigma_{\alpha\beta}$, the associated stress or dynamic strength listed in Table 1, and substituting the remaining dynamic properties from Table 1, R in Equation 11 becomes $R_{\alpha\beta}$, the distance to the end of the transition boundary shown as

$$22 = 48\sqrt{\frac{26}{R_{\alpha\beta}}}e^{-(R_{\alpha\beta}-26)(0.03)}$$

This equation is also solved numerically giving the final distance of damage caused by the radial compressive stress, $R_d = 44$ cm.

The decay of stress in the seismic zone causes no damage and is given by,

$$\sigma = \sigma_{\alpha\beta}\sqrt{\frac{R_d}{R}}e^{-(R-R_d)\alpha} \tag{12}$$

Where α = seismic decay (1/cm). Substitution of the seismic properties from Table 1 and the final damage distance into Equation 12 gives,

$$\sigma = 22\sqrt{\frac{44}{R}}e^{-(R-44)(0.0005)}$$

Figure 9 presents a semi log plot of calculated stress vs. distance for the concrete block experiment using the piecewise continuous functions. The extensive damage zone extends to a distance of 26 cm from the center of the blasthole. The final damage extends to a distance of 44 cm from the center of the blasthole. Beyond 44 cm the model is seismic and no damage is computed. Note that the NIOSH stress decay method does not include the damage from the expanding explosive gas but only describes the damage caused by the compressive stress wave.

4.3 *Drukovanyi stress approach*

Drukovanyi et al. (1976) investigated the process of fracture of brittle rock for a quasi-static expansion of detonation gases in a cylindrical cavity. They assumed an axi-symmetric plane of deformation and three zones including fine crushing, radial cracking, and an elastic zone. According to Drukovanyi, the boundaries are determined according to Rodionov et al. (1971) as follows:

The fine crushing zone

$$a_0 \le r < b_* \tag{13}$$

The radial fissure zone

$$b_* \le r < b_0 \tag{14}$$

The elastic fissures zone

$$b_0 \le r < \infty \tag{15}$$

where r = distance from the charge, a_0 = radius of the expanding cavity, b_* = radius of the crushed zone, and b_0 = inner boundary of the elastic zone.

Drukovanyi et al. (1976) theoretically derived the extent of the crushed zone as:

$$b_* = a_0\left[\frac{P_e}{\frac{-C}{f}+\left(\sigma_c+\frac{C}{f}\right)L^{\frac{f}{1+f}}}\right]^{\frac{1}{2\gamma}}\sqrt{L} \tag{16}$$

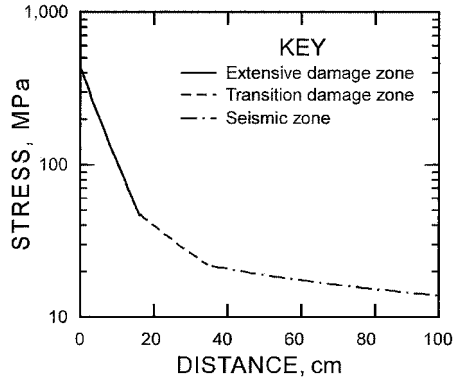

Figure 9. Calculated stress in the concrete block using the decay of compressive stress method.

$$L = \frac{\mu}{\sigma_c\left(1 + \ln\frac{\sigma_c}{\sigma_t}\right)} \quad (17)$$

$$\mu = \frac{E}{1+\nu} \quad (18)$$

where C = cohesion of rock, f = coefficient of internal friction of rock, σ_c = uniaxial compressive strength of rock, σ_t = tensile strength of rock, E = Young modulus, ν = Poisson's ratio, μ = Lame's coefficient, and γ = ratio of specific heats.

Drukovanyi et al. (1976) derived the extent of the radial fissure zone as

$$b_0 = \left(\frac{\sigma_c}{\sigma_T}\right) b_* \quad (19)$$

Based on the physical properties listed in Tables 1 and 2, b_* and b_0 were determined to be 33 cm and 396 cm, respectively. The fine crushing zone, b_* was less than the measured crush distance of 50 cm. The radial fissure zone, b_0 exceeded the actual radial crack limit by over a factor of 2.

4.4 *NIOSH-modified Holmberg-Persson model*

The Holmberg-Persson perimeter blast design approach has found widespread use since its introduction in 1978 (Holmberg & Persson 1978, 1979). It is logical and easy to apply. Unfortunately, a recently discovered mistake in the equation development has raised questions regarding the whole procedure (Hustrulid & Lu 2002). The Holmberg and Persson expression is an integration over the charge length for a charge concentration identified over z initial (z_i) to z final (z_f) as

$$PPV = K\left\{q\int_{z_i}^{z_f} \frac{dz}{[(r-r_0)^2 + (z-z_0)^2]^{\beta/2\alpha}}\right\}^{\alpha} \quad (20)$$

where PPV = peak particle velocity, K = constant, q = charge concentration (kg/m), α = constant, β = constant, r = element radial location (m), z = element location along the charge (m), r_0 = radial measure point (m), and z_0 = longitudinal measure point (m).

NIOSH has reviewed the basics of the Holmberg-Persson design approach and introduced a modification which retains the simplicity of the procedure while correcting the mathematical problems (Iverson et al. 2008). This new theoretical approach is based on first determining the average distance from the charge to the measure point. The average distance is then inserted into the charge weight inverse distance equation for PPV. The basic equation is

$$PPV = K\frac{Q^{\alpha}}{\bar{R}^{\beta}} \quad (21)$$

where Q = total charge weight, kg, and $\bar{R}$ = average travel distance.

The average wave travel distance, $\bar{R}$ is by definition (Iverson et al. 2008),

$$\bar{R} = \frac{1}{L}\int_{z_i}^{z_f}\left[(z-z_o)^2 + (r-r_o)^2\right]^{1/2} dz \quad (22)$$

where L = charge length ($z_f - z_i$), m.

This $\bar{R}$ method is adequate for predicting the PPV at points located at distances greater than 1 m. This method, however, underestimates the PPV at points at distances les than 1 m. An improved calculation of $\bar{R}$ is to use an inverse distance weighting to the power of β (Shepard 1968) and weight the distance for each element of the charge. This weighting approach results in a design curve that compares closely with the Holmberg-Persson integration design curve with assurance that a math error is not introduced.

The NIOSH-modified equation is useful for calculating PPV values near the charge and predicting damage. In practice, one develops the PPV vs. distance curves for the explosive concentrations of interest. The curves are fit to the site data by adjusting the constants α, β, and k. One then measures the rock damage limits such as the crush zone, overbreak zone, and the radial crack zone for each explosive type. Using the damage limits and the PPV vs. distance design curves, one can determine the limiting PPV for each damage zone. One now has a practical design tool for the site.

In applying this approach, the block test PPV values based on the measured radial strains are plotted in Figure 10 with the NIOSH-modified PPV equation fit. The site constants $\alpha = 1.2$, $\beta = 2.4$, and $K = 0.65$ were determined. These constants vary considerably from constants determined by Lundborg et al. (1978). In analyzing the results of a large set of surface blasting measurements performed by the U.S. Bureau of Mines, Lundborg found that the site constants are well described using $\alpha = 0.7$, $\beta = 1.5$, and $K = 0.7$. For comparison, the Holmberg-Persson equation is also plotted in Figure 10 using these Lundborg constants. Obviously, the Lundborg constants do not adequately describe the block test data in magnitude or attenuation. For the Lundborg plot, a simplified solution to the Holmberg-Persson integration was used where the $\alpha/\beta = 0.5$. Therefore, an α value of 0.75 was used to maintain the 1.5 value for β.

Design curves based upon the NIOSH-modified equation for a range of Dyno® AP charge concen-

trations are shown in Figure 11. The crush and radial crack damage PPV limits are compared to the design curve charge concentrations. The limiting PPV values are 3.9 m/sec and 0.29 m/sec, respectively. The curves represent PPV values vs. distance for a charge length of 1.22 m at predicted radial distances from the charge midpoint.

4.5 *Hydrodynamic approach*

The application of hydrodynamics to calculate theoretical velocity components at a given distance from a fully-coupled charge was pioneered and published in Russian by Vlasov, Smirnov, Kuznetsov, Illushyii, Krasov, Neyman and others. Design curves can be constructed for a given rock mass by calibrating the theoretical velocity values using measured velocity and distance data from a single-charge test. Hustrulid subsequently presented Neyman's work in English. This methodology follows.

For velocity u perpendicular and midheight to a charge of length L and diameter d, the theoretical velocity equations developed by Neyman and others can be simplified to Equation 23.

$$u = I\,\rho^{-1} \tag{23}$$

where

$$I = \sqrt{\frac{\rho_e\, q_e}{8\rho_m}} \tag{24}$$

where ρ_e is the density of the explosive, q_e is the specific energy of the explosive, ρ_m, is the density of the medium,

$$\rho = \frac{\sqrt{v_s}\,\bar{r}\sqrt{\bar{r}^2 + \frac{\bar{L}^2}{4}}}{\bar{L}} \tag{25}$$

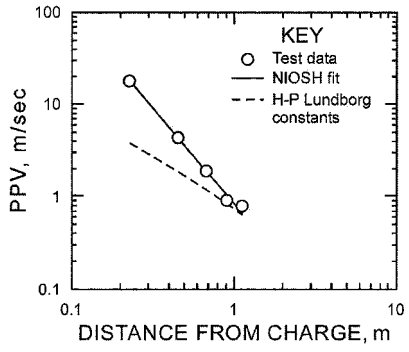

Figure 10. Comparison of block test PPV data, the fit NIOSH-modified equation using constants $\alpha = 1.2$, $\beta = 2.4$, and $K = 0.70$, and the Holmberg-Persson integration using the poorly fit Lundborg et al. (1978) constants.

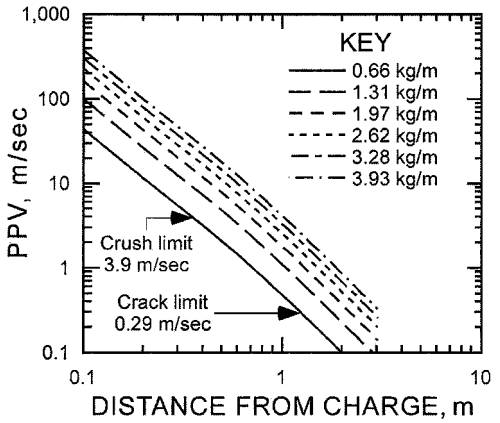

Figure 11. NIOSH PPV design curves for Dyno® AP in tested concrete for a range of charge concentrations and two damage limits.

where

$$v_s = \ln\frac{\bar{L} + \sqrt{1+\bar{L}^2}}{-\bar{L} + \sqrt{1+\bar{L}^2}} \tag{26}$$

$$\bar{L} = \frac{L}{d} \tag{27}$$

$$\bar{r} = \frac{r}{d} \tag{28}$$

Theoretical velocity expressed as a function of ρ for the SRL block test parameters is

$$u = 482\,\rho^{-1} \tag{29}$$

and is plotted in Figure 12.

Neyman shows that field data have the same form as Equation 23, but with a different coefficient and exponent for ρ. For the SRL concrete block test, the equation is:

$$u_m = 414\,\rho^{-1.416} \tag{30}$$

where u_m is measured velocity. Measured velocity versus ρ for the SRL block test is shown in Figure 12.

A calibration equation that relates field velocity to theoretical velocity is obtained by dividing Equation 29 by Equation 30 which yields

$$\frac{u}{u_m} = 1.16\rho^{0.416} \tag{31}$$

Equation 31 can be used to create design curves with various charge diameters for the medium in

which the test was conducted. Figure 13 is a plot of PPV versus distance for a 1.2-m long by 38-mm diameter cylindrical charge. The PPV values for distances of 0.5 and 1.8 m are approximately 4.5 m/s and 0.2 m/s, respectively.

5 CONCLUSIONS

The concrete block experiment results indicate a crush limit on the order of 50 cm measured radially from the center of the column charge and a crack limit extending to 176 cm. The crush limit was based on MVP s-wave, cross-core seismic p-wave, and splitting tensile strength measurements. The crack limit was measured from visual inspection of wire saw cut surfaces. These damage limits are specific the concrete material and the Dyno® AP explosive tested.

Five different blast models were assessed. Three of the blast models, the modified-Ash, the NIOSH stress decay, and the Drukovanyi stress, provided specific damage types and limits. These are summarized in Table 4.

The NIOSH-modified Holmberg-Persson approach was applied to the PPV test data. Design curves for various charge concentrations were developed illustrating that an increase in charge concentration will result in increased crush and radial crack damage.

Hydrodynamic theory produces a simplified equation for cylindrical charges that relates theoretical PPV to distance from a charge for a given explosive and rock mass. This equation was calibrated using data from the concrete block. The PPV limit corresponding to a damage of 50 cm was 4.5 m/s and the crack limit of 176 cm, it was 0.28 m/s.

At this point in time, it appears that the most promising of the blast damage models evaluated

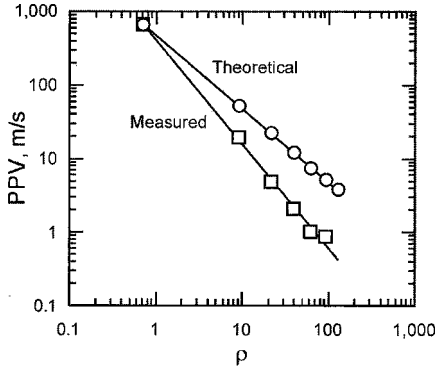

Figure 12. Theoretical and measured velocity versus ρ for block test.

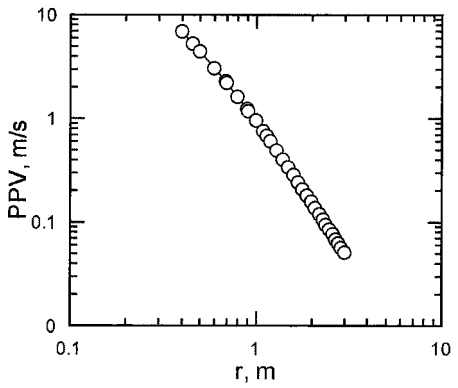

Figure 13. PPV versus distance from charge for a 1.2-m long, 38 mm diameter charge.

both from the ease of calculation and the resulting practical damage limit is the modified-Ash method. The other models require rock physical property testing or on-site blast vibration measurements. The authors believe that the crush and crack limits in themselves are not practical for design purposes. The practical damage limit must lie somewhere in-between. Figure 14 illustrates the application of the modified-Ash method and evaluated damage limits to fully-coupled perimeter holes in a 4 m by 4 m drift. This design would be considered aggressive blasting and typically results in over-break damage. The crack damage in Figure 4 has been applied to the drift design in Figure 14. The maximum damaged perimeter, according to the modified-Ash method, extends 87 cm into the rock mass.

Burden can have a significant affect on perimeter damage. In the block experiment, the burden was 45 cm. Interestingly, the crush damage limit was nearly the same at 50 cm. The authors believe there may be a relationship between burden and perimeter damage due in part to duration of explosion pressure. Burden affect is discussed in Hustrulid & Iverson (2009).

This research has identified a number of critical issues that must be addressed and resolved including:

- Need for good definition of types of damage and how they should be included into the blast design.
- How should practical damage be defined and how should it be measured.
- Are damage calculations to be based on wave energy, gas pressure, or both?
- Are quasi-static methods adequate or are dynamic approaches needed.
- Do we need static or dynamic properties in the models?

Table 4. Summary of damage limits calculated based on the block test properties using various blast models.

Blast model	Damage limit, cm	Damage type*	Damage mechanisms
modified-Ash, energy-based	61	Practical	Energy
modified-Ash, pressure-based	87	Practical	Quasi-static pressure
NIOSH stress decay	26	Extensive crushing	P-wave
NIOSH stress decay	44	Transition	P-wave
Drukovanyi stress	33	Crush	Quasi-static pressure
Drukovanyi stress	396	Radial cracks	Quasi-static pressure

* damage type as defined by the blast model.

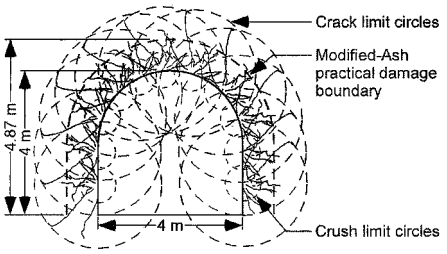

Figure 14. Hypothetical 4 m × 4 m drift round in tested material showing crush, crack, and practical perimeter damage limits.

- For dynamic properties, how do we get them? What tests should be used.
- Are basic explosive properties adequate for the blast models? If not, what is the practical alternative?

The goal of this research to develop simple, yet technically sound blast damage models which can be incorporated into a user-friendly careful blasting design software tool "Drift" under development by NIOSH. This tool would help engineers design blasts resulting in less perimeter damage, reduced scaling requirements, and improved ground quality. These benefits translate into reduced exposure to injuries from roof or rib ground falls, thus improving the safety of the miner.

ACKNOWLEDGEMENTS

This work could not have been accomplished without the help of Carl Sunderman, Ron Jacksha, Mike Stepan, Ted Williams, Edward McHugh, Paul Pierce, Ken Strunk, and Mark Johnson.

REFERENCES

ASTM. 2001. D 3967 Standard Test Method for Splitting Tensile Strength of Intact Rock Core Specimens. *American Society for Testing and Materials.*

Drukovanyi, M.F., Kravisov, V.S., Chernyavskii, Y.E., Shelenok, V.V., Reva, N.P. & Zver'kov, S.N. 1976. Calculation of fracture zones created by exploding cylindrical charges in ledge rocks. *Soviet Mining Science* 12(3): 292–295.

Dyno Nobel. 2009. DYNO® AP, Small diameter Detonator Sensitive Emulsion. *Dyno Nobel P-08-08-20-07*, http://www.dynonobel.com/NR/rdonlyres/C2C07E5B-C82F-4AC5-ACF4-E671410197AA/0/Dyno_AP.pdf

Holmberg, R. & Persson, P.A. 1978. The Swedish approach to contour blasting. *Proceedings of the 4th Conference on Explosives and Blasting Technique*, New Orleans, February 1–3, ISEE, pp 113–127.

Holmberg, R. & Persson, P.A. 1979. Design of tunnel perimeter blasthole patterns to prevent rock damage. In M.J. Jones (ed.), *Proceedings, Tunneling '79*. London, UK: Institution of Mining and Metallurgy.

Hustrulid, W. 1999. *Blasting Principles for Open Pit Mining Volume 2–Theoretical foundations*. Rotterdam: Balkema. 631 pp.

Hustrulid, W.A. & Iverson, S.R. 2009. Evaluation of Kiruna mine drifing data using the NIOSH design approach. In J.A. Sanchidrián (ed.), *Proceedings of the 9 International Symposium on rock Fragmentation by Blasting (FRAGBLAST 9)*, Granada, Spain, September 13–17. Rotterdam: Balkema.

Hustrulid, W. & Johnson, J. 2008. A gas pressure-based drift round blast design methodology. In H. Schunnesson & E. Nordlund (eds.), *Proceedings of MASSMIN 2008, 5th International Conference & Exhibition on Mass Mining*, Lulea, Sweden, 9–11 June 2008. Lulea University of Technology, pp. 657–669.

Hustrulid, W. & Lu, W. 2002. Some General Design Concepts Regarding the Control of Blast-Induced Damage During Rock Slope Excavation. *Proceedings, FragBlast7*, Beijing, China, August 11–15.

Iverson, S., Kerkering, C. & Hustrulid, W. 2008. Application of the NIOSH-Modified Holmberg-Persson Approach to Perimeter Blast Design. *Proceedings of the 34th Annual Conference on Explosives and Blasting Technique*, New Orleans, Louisiana, January 27–31.

Johnson, J.C. 2009. *The Hustrulid Bar—A Dynamic Strength Test and its Application to the Cautious Blasting of Rock*. PhD dissertation, University of Utah, Department of Mining Engineering, 400 pp.

Lundborg, N., Holmberg, R. & Persson, P.A. 1978. The dependence of ground vibrations on distance and charge size. Report R11:78. Byggforskning. In Swedish.

McCarter, K. 2006. Personal communication. University of Utah.

Rodionov, V.N., Adushkin, V.V., Kostyuchenko, V.N., Nikolaevskii, V.N., Romashev, A.N. & Tsvetkov, V.M. 1971. Mechanical Effects of an Underground Explosion, *Izd-vo Nedra*. Moscow. In Russian.

Shepard, D. 1968. A two-dimensional interpolation function for irregularly-spaced data. *Proceedings of the 1968 23rd ACM National Conference*, New York, August 27–29, pp. 517–524.

PROCEEDINGS OF THE 9TH INTERNATIONAL SYMPOSIUM ON ROCK FRAGMENTATION BY BLASTING – FRAGBLAST 9, GRANADA, SPAIN, 13–17 SEPTEMBER 2009

Rock Fragmentation by Blasting

Editor

José A. Sanchidrián

Universidad Politécnica de Madrid, Madrid, Spain

CRC Press

Taylor & Francis Group

Boca Raton London New York Leiden

CRC Press is an imprint of the

Taylor & Francis Group, an **informa** business

A BALKEMA BOOK

5 *Rock damage and wall control*